



## Effect of Including Periodic Boundary Condition on the Fatigue Behaviour of Cancellous Bone

Fatihhi Januddi<sup>1\*</sup>, Muhamad Noor Harun<sup>2,3</sup>, Ardiyansyah Syahrom<sup>2,3</sup>, Adnan Bakri<sup>1</sup>, M. F. M. Alkbir<sup>1</sup>

<sup>1</sup>Advance Facilities Engineering Technology Research Cluster (AFET-RC)  
Facilities Maintenance Engineering Section (FAME), Malaysian Institute of Industrial Technology,  
Universiti Kuala Lumpur (UniKL MITEC), Persiaran Sinaran Ilmu, Bandar Seri Alam, 81750, Johor, MALAYSIA

<sup>2</sup>Medical Devices and Technology Centre (MEDITEC), Institute of Human Centred and Engineering (iHumEn),  
Universiti Teknologi Malaysia, 81310, Johor, MALAYSIA

<sup>3</sup>Department of Applied Mechanics & Design, School of Mechanical Engineering, Faculty of Engineering,  
Universiti Teknologi Malaysia, Skudai, 81310, Johor, MALAYSIA

\*Corresponding Author

DOI: <https://doi.org/10.30880/ijie.2020.12.05.009>

Received 21 May 2020; Accepted 28 May 2020; Available online 30 June 2020

**Abstract:** Trabecular bone consists of complex webbing of plates and struts, in which the properties vary across anatomical sites. The substantial constraint is the reduction on discretization error will reduce time in computation. So it is significant to consider carefully the boundary condition effects when utilizing such a complex multiaxial loading mode. Additionally, multiaxial loading gives distinct effects towards boundary condition compare to uniaxial whereas percentage prediction of fatigue failure is lower and applying of periodic boundary reflect a more precise real loading condition. 3D models of trabecular samples were constructed for FE simulations. The response of the models towards simulated mechanical loading was investigated. Preparation of the models begins with 3D reconstruction of micro-CT stacked images, follows by segmentation, meshing and refurbishing process. The resistance of trabecular bone deformation to loading in both uniaxial and multiaxial modes improved the fatigue life and failure with application of periodic boundary conditions.

**Keywords:** Periodic boundary; Fatigue; Cancellous Bone; Multiaxial; Mechanical behavior

### 1. Introduction

For over 30 years, biomechanics research has been widely explored with special interest is sending forth on the influence of trabecular bone towards weakening and failure of whole bone, and how the stimulating remodeling process helps in retaining the bone strength. Clear understanding of the biomechanics of bone is well related in diagnosis and treatment of medical issues such as osteoporosis, bone fracture, bone remodeling, and implant system.

Fracture in bone [1,2], age-related fragility fractures [3] and implants loosening [4] have been found to be originated by fatigue damage. However, fatigue behavior of trabecular bone has received only few attentions [5–8]. Even so, these studies are conducted under uniaxial compressive loading, in which may badly aligned with in vivo physiological off-axis loading directions [7]. This off-axis loading is influenced by trabecular micro architectural properties, which are also attributed to osteoporosis. Thus, understanding the fatigue properties of bone may provide information on osteoporotic bone behavior toward normal physiological loading and its associated diagnosis and treatment, as well as improve implant systems in terms of material selection, placement and interface mechanism.

\*Corresponding author: [mohdalfatihhi@unikl.edu.my](mailto:mohdalfatihhi@unikl.edu.my)

2020 UTHM Publisher. All rights reserved.

[penerbit.uthm.edu.my/ojs/index.php/ijie](http://penerbit.uthm.edu.my/ojs/index.php/ijie)

Trabecular bone consists of complex webbing of plates and struts, in which the properties varies across anatomical sites. Reconstruction of the whole trabecular model for computational analysis can benefit the research in bone pathology and clinical applications. However, due to limitation in equipment and the complexity of the trabecular structure itself, the reconstruction process for the whole model is highly unfeasible. Thus, this study aims to extract only a small sub volume region of interest to predict the uniaxial and multiaxial stress response and behavior of the whole trabecular structure which is never been done before. Several models are presented in current study with different morphological parameters to see these effects. The mechanical properties and fatigue response of these models are evaluated and compared. The validation of FEA with experimental results was also included to ensure the simulation accuracy of the developed model. Further, the effect of the applied periodic boundary on the assessed models was investigated.

## 2. Methodology

### 2.1 Experimental Setup

For mechanical testing, the extremities of each sample were fixed to stainless steel end caps with adhesives [9,10]. The end caps were then placed inside a jig (Fig. 1) to achieve perfect alignment to the vertical axis of the universal testing machine and thus removed end artefacts [11]. Once placed inside the jig, a spring is used to ensure that the extremities of the sample filled the opening of the end caps completely. The extent of the hot-melt adhesives (DGHL, model HL-E, China) covered approximately 5 - 7 mm from both extremities of the samples for compression testing, reducing the effective length of the samples from 25 mm to 15 mm.

Additionally, fitting of the samples for torsion testing was further assured by mounting the samples extremities with polymer mixture of resin and hardener of 5000 MPa in strength (UNI-LAB & CO, GmbH). The sample was cold mounted properly in hardened mixture and cured for 24 hours. The alignment between polymer and samples was secured using a custom rig (Fig. 1 (a)) to reduce error and artefacts during testing [12]. The mounted polymer covered approximately 7 - 10 mm of the sample length from its extremities, reducing the effective length of 40 - 35 mm to 15 - 20 mm. The average sample diameter was 9.86 - 10 mm. The polymeric extremities were cut (Allied precision diamond cutter, USA) to be fitted and secured inside the jig which was clamped into the hydraulic wedge grips (Fig. 1 (b)). The lower grip was fixed while the upper grip was fluctuated and rotated.

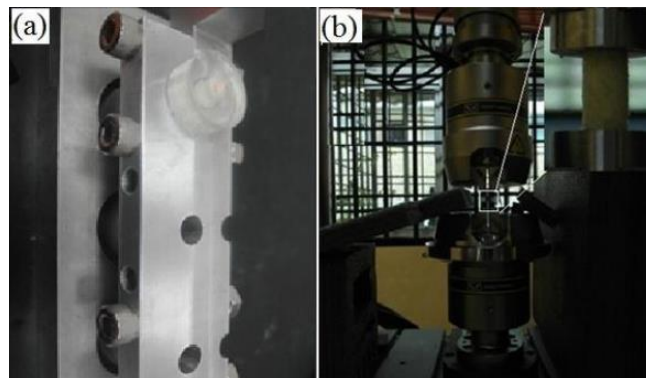


**Fig. 1 - Mechanical testing setup for (a) samples alignment; (b) universal testing machine with a sample attached**

A total of 73 samples were used for uniaxial compression and combined loading compression-torsion fatigue testing. Tests were conducted in the same condition as per monotonic test with separated load cell (Biaxial Dynacell™). This dynamic load cell has load capacity of 25 kN, torque capacity of 100 Nm and 0.5% precision from 1% of the full scale.

### 2.2 Computational Analysis

3D models of trabecular samples were constructed for FE simulations. The response of the models towards simulated mechanical loading was investigated. Preparation of the models begins with 3D reconstruction of micro-CT stacked images, follows by segmentation, meshing and refurbishing process.

In the simulation part, COMSOL 4.3 (COMSOL Inc., Burlington, USA) was used to run the FE analysis which coupled with Matlab pre-processing and post processing. Integration of COMSOL with MATLAB thereby extending COMSOL's simulation tools with scripting capabilities. This allows for saving COMSOL models as M-files. COMSOL generated M-files can be combined with any MATLAB M-files for advanced post-processing, statistical and probabilistic analysis, for-loops, optimization, and combination with other MATLAB add-on tools. After mesh surface

editing, the reconstructed models were converted to FE mesh. Due to computational limitation for high-resolution models, only the small size of sub volume in region of interest (ROI) in trabecular model was selected for FE simulation.

The model was assigned to be homogeneous and isotropic with linear elastic properties. The Young's modulus value was set to 1000 MPa. The Poisson's ratio of 0.3 was specified with regard to the trabecular apparent density of 1 g/cm<sup>3</sup> [13,14]. As the models were small in size, periodic boundary conditions were implemented thus a model was assumed as repeated unit cells arranged in period of infinite number [14]. This repetitive symmetry condition was achieved by multiple point constraint with similar x-displacement nodes on the surface of the model as shown in Fig. 2. This modelling technique requires macroscopic displacements parallel to the x- and y-axes in order to fulfil reflective symmetry of the loads [13,14].

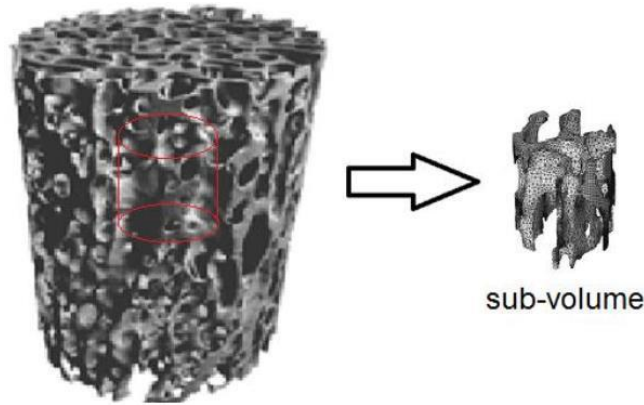


**Fig. 2 - Reconstructed 3D trabecular bone model being excised to sub-volume ROI which high in resolution but small in size**

### 3. Results

Morphological analyses on trabecular bone samples give measurement on the morphological indices. Bone volume fraction ranged from 33.50 to 47.00 % ( $42.12 \pm 5.26$  %). Trabecular thickness (Tb.Th) mean value was 0.243 mm, within the range of 0.214 mm to 0.29 mm. The range for the distance between the trabeculae, trabecular separation (Tb.Sp) was measured to be in between 0.356 mm and 0.565 mm. Bone volume fraction (BS/TV) and bone surface fraction (BS/BV) both were recorded with average values of 0.194 and 0.198, respectively. The rod- versus plate-like type of structure which was indexed by the value of SMI averaged at 0.651. The connectivity density of the trabecular samples denoted as Conn.D was 5.03/mm<sup>3</sup> in average, best suited to the ranged reported in previous work [13,15]. The convergence study was included and the chosen mesh density was chosen consistent to that of previous section Fig. 3. The convergence is considered successful with less than 10% difference. The number of elements in FE models range from 408,571 to 1,004,996 elements.

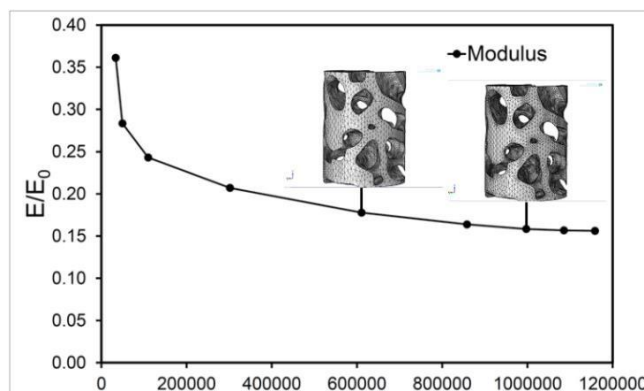


**Fig. 3 - Convergence behavior of trabecular bone model relationship between normalized Young's modulus with number of elements**

Correlation with the experimental data and prediction of fatigue life under the applied stress are shown in Fig. 4. Good agreement is observed in between the computational predictions with periodic boundary and the experimental analyses with less than 10% differences for modulus.

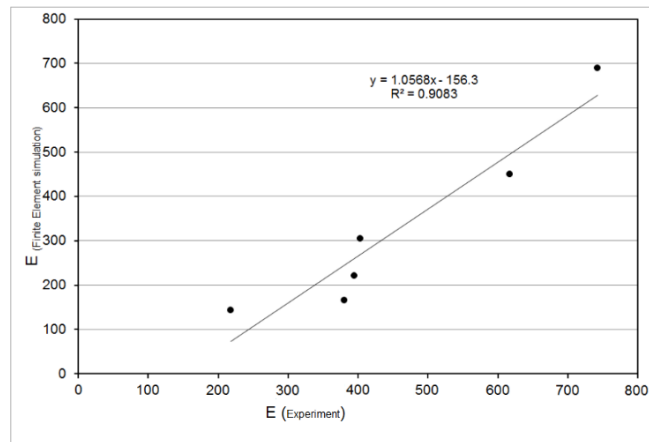


**Fig. 4 - Comparison between FE simulation and experimental modulus with periodic boundary condition**

The effect of periodic boundary on fatigue life prediction of trabecular bone model is shown in Fig. 5. The effective von-Mises stress was measured through minimum surface reached the predefined critical value. Similar trend is observed in the stress-cycle fatigue for models analyzed both with and without periodic boundary. Fatigue life is shown decreases with increase stress. However, fatigue cycles for models without periodic boundary were lower than that of models with periodic boundary. Good correlation was found in between the models both with and without periodic boundary and can be easily depicted from the stress-life curve. High errors of 92% in average denoted significant difference between both conditions ( $p < 0.05$ ). In overall, 54% average in fatigue strength coefficient between the two conditions were found, where the models without periodic boundary underestimate the fatigue life at 1.2 times in comparison to the models with periodic boundary.

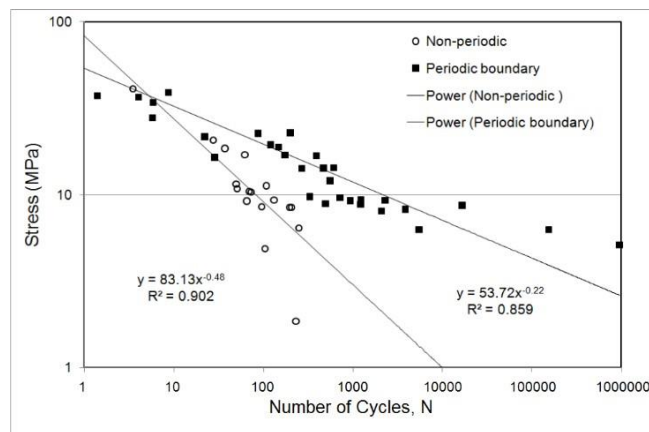


**Fig. 5 – Effect of periodic and non-periodic boundary on the fatigue life evaluation of trabecular bone models**

Comparison on the effect of periodic boundary in between models under uniaxial loading and multiaxial loading shows smaller value of cycles to failure in models without periodic boundary for both loading conditions (Fig. 6). Further, lower effective plastic strain is observed for models under uniaxial loading in both with and without boundary conditions, as depicted in (Fig. 7). On the other hand, the strain is observed to be slightly higher for the models under multiaxial loading in all cases.

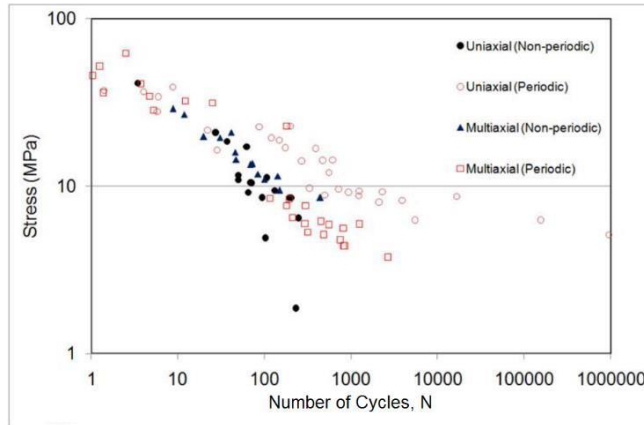


**Fig. 6 - The S-N relationship of simulation models subjected to uniaxial and multiaxial loading with and without periodic boundary condition**

Fig. 8 shows the percentage difference of the calculated mechanical parameters from FE simulation from models with and without boundary condition under both uniaxial and multiaxial loading. This percentage difference is in between models with periodic boundary conditions and models without periodic boundary condition. Distinctive trend in percentage difference of von-Mises stress and volumetric strain is noticed, with higher von-Mises stress mean value for models under uniaxial loading without boundary condition in comparison to those under multiaxial loading (Fig. 8 (a)). The percentage difference of von-Mises stress for models under uniaxial and multiaxial loading were  $110 \pm 42.26\%$  and  $68.35 \pm 51.34\%$ , respectively. However, the percentage difference of volumetric strain was found to be slightly higher in models under uniaxial loading than that of multiaxial loading (Fig. 8 (b)).

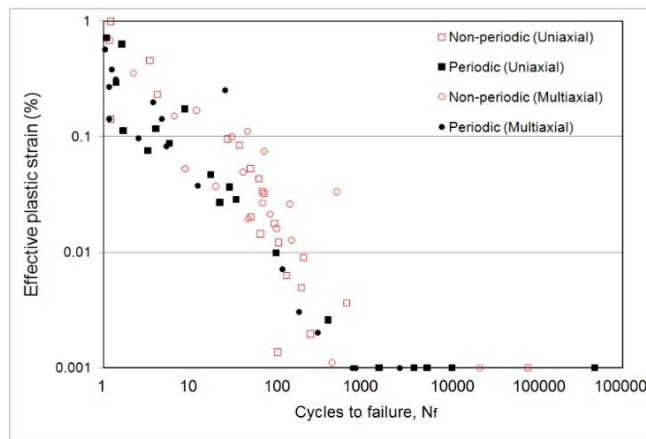


**Fig. 7 - Strain to cycles to failure relationship of simulation models subjected to both uniaxial and multiaxial loading based on normal walking with and without periodic boundary condition**

Stress concentration is observed only in sample without periodic boundary under multiaxial loading (Fig. 9 (a)). More deformation can be seen in the model without application of periodic boundary. Compared to model with imposed of periodic boundary, different maximum stress distribution on the trabecular surfaces due to different boundary conditions.

Fig. 10 shows the percentage difference of the calculated cycles to failure,  $N_f$  from FE simulation from models with and without boundary condition under both uniaxial and multiaxial loading. This percentage difference is in between models with periodic boundary conditions and models without periodic boundary condition. Same trend in percentage difference is noticed, with another different value for models under uniaxial loading without boundary condition in comparison to those under multiaxial loading. The percentage difference of for models under uniaxial and multiaxial loading were 97% and 67%, respectively. Overall, the average of cycles to failure in all boundary condition is shown in Fig. 11. The uniaxial loading with periodic boundary was found to be higher in all models where lowest for multiaxial loading without periodic boundary condition.

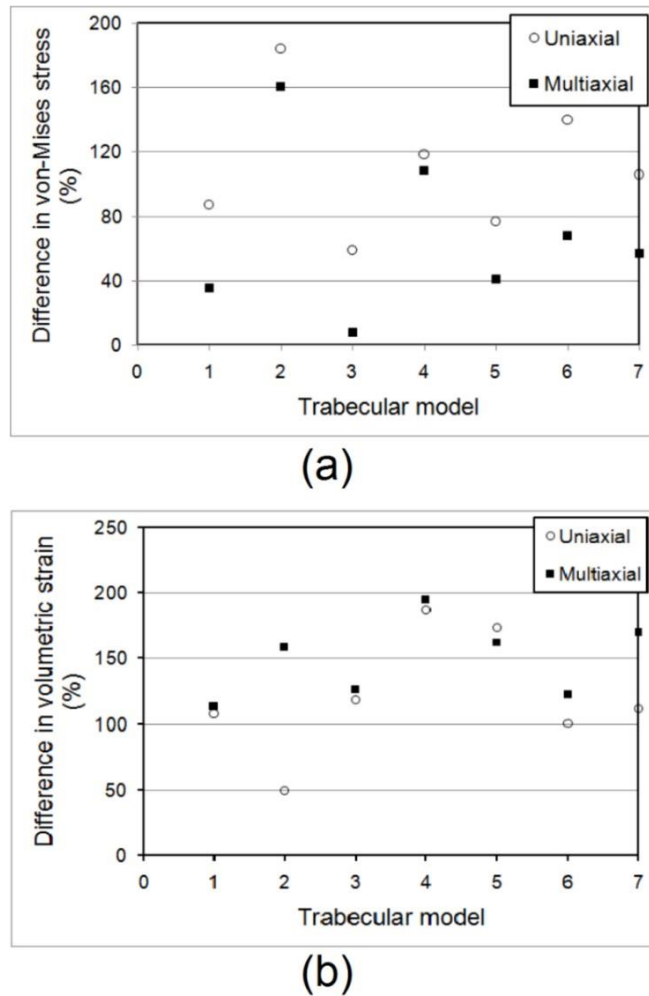


**Fig. 8 – The difference in (a) von-Mises stress; (b) volumetric strain for with and without periodic boundary condition models subjected to both uniaxial and multiaxial loading**

#### 4. Discussion

Experimental results show good qualitative low cycle fatigue (LCF) and high cycle fatigue (HCF) separation which was explained previously in the literature [13,16]. LCF and HCF profile can be combined generally and be assumed as the effective strain under general strain-life curve. The results can be affected by inclusive tissue heterogeneity based on the mineralization level [17]. However, consideration on the model homogeneity properties is only appropriate in the analyses of human bone. The model reconstructed from bovine trabecular bone in present study is relatively a plate-like structure [18], thus can be assumed to be isotropic. Stress-strain field of the trabecular is determined by FE analyses, in which the prediction of mechanical parameters and fatigue life is investigated. Further, this study contributes to the evaluation of bone fracture risks under physiological loading conditions, in which the loading is not restricted to uniaxial loading.

Trabecular bone fracture has been recognized to be initiated at the trabecular scale with high stress or strain [19]. Besides, it is known that during habitual loading, the biological response is triggered by the mechanical stress [20,21]. This study shows the higher value of elastic modulus and yield strength in models from femoral ball than those from condyle which can depend on the high volume fraction and bone surface density. This is due to high composition of plate like trabecular. Increase of strength across medial-lateral condyle to femoral ball is observed due to the differences in trabecular structure across different anatomic sites [22] as well as regional variations [23]. Differences of elastic modulus across anatomic sites are especially higher in proximal femur owing to its density which gives it the higher strength than in other anatomic sites [24,25]. Furthermore, in vivo loading condition bear during habitual activities varied across different anatomic sites, thus generate diverge local density and microarchitecture changes.



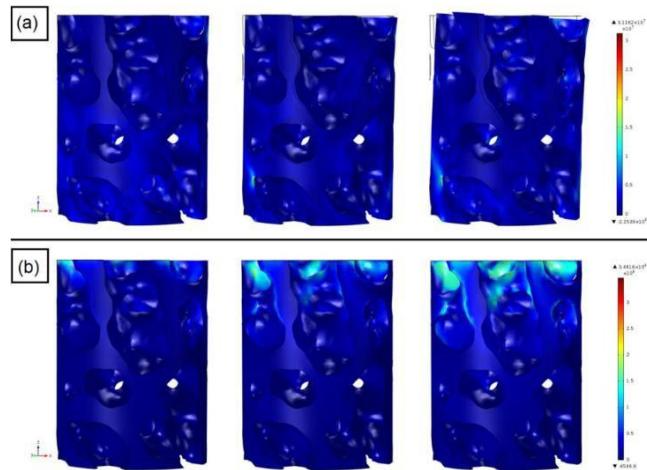


**Fig. 9 - Microstructural model deformations with: (a) without periodic boundary; (b) when periodic boundary conditions are imposed on the trabecular structure**

Medial compartment of the condyle sustained greater load during normal walking than the lateral compartment [26,27], thus may influence the morphological structure properties and subsequently affect its elastic properties and yield behavior. Buckling during compression and necking during tensile give obvious variation on yield stress distribution between rod- and plate-like trabecular. Buckling has also been reported to affect rod-like trabecular in experimental investigation [28]. Orientation of strut following principle loading axes results in the worst case in comparison to the horizontal struts. This shows that the initiation of yielding in trabecular does not only depend on the type of trabecular yet influenced by struts orientation. This is supported by previous finding which shows the plate-like trabecular dominated the elastic modulus in trabecular bone than that of rod-like trabecular [29]. The combined effect of trabecular separation with struts breakage in a small fragment could result in lower elastic and strength even plates are more pronounce in specific site than rod-like trabecular.

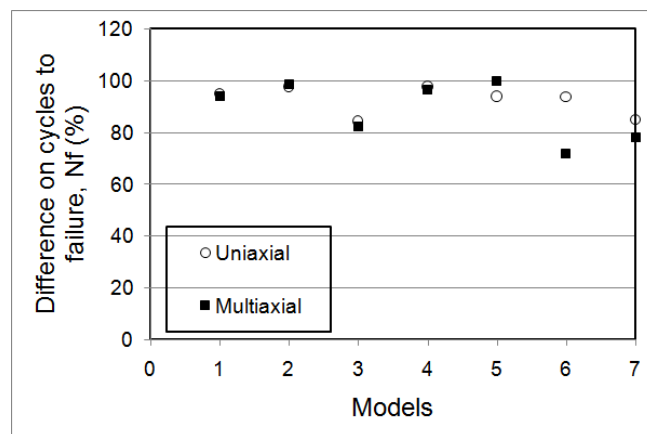


**Fig. 10 - Difference in cycles to failure prediction of trabecular FE model under uniaxial and multiaxial loading conditions with respect to periodic boundary**

In this study, the uniaxial and multiaxial with specific micro architectural parameters difference were used to predict the failure and effective plastic strain. Traditionally, to diagnose vertebral osteoporosis, BMD is measured. However, this method fails to account the changes in the trabecular bone and quantify how this changes affect the quality of the trabecular [30,31]. Age-related changes of the trabecular bone included a decrease in BV/TV and Conn.D, an increase in Tb.Sp, a shift from plate-like trabecula to a rod-like structure [27,30,32]. An estimation of plate or rod characteristic of trabeculae can be explained with measuring SMI. SMI is highly dependent on trabecular type (plate- to rod-like structure) thus the mechanical behavior can be predicted under both uniaxial and multiaxial loading. Change in the type of trabecular structure is well related to age [23,33].

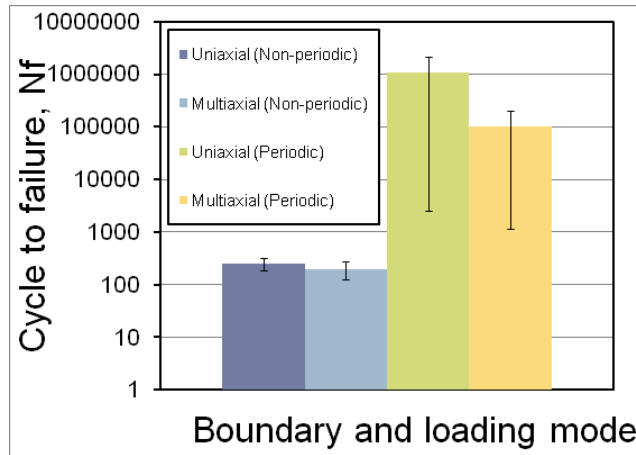


**Fig. 11 - Mean values of cycles to failure with different type of boundary condition and loading mode**

This study shows a significant effect of this parameter to fatigue life which contributes to the strength of the trabecular structure. In both loading conditions, low-SMI demonstrated high endurance towards fatigue loading. On the contrary, fatigue life cycles decreased significantly in samples with high-SMI. However, increase in effective plastic strain is also observed in some cases with low cycle fatigue. As the sample’s structure is dominated by rod-like trabeculae, the ability of the sample to sustain prolonged loading is reduced. BV/TV and Conn.D values affect the fatigue life of the trabecular bone under multiaxial loading significantly. Severe shear effect could be associated to the reduction of fatigue life in which alteration on trabecular orientation can be seen. In comparison to the samples under uniaxial loading, the horizontal trabecular struts are less affected in which most of the load was bore on vertical struts. Thus, the sample failed by bending. This condition is closely associated with the thinning of the trabecular and an increase in anisotropy with increasing age in osteoporotic bone. However, under multiaxial loading, the trabecular structure was loaded in multiple directions in which resulting in failure of the struts irrespective to its orientation. High bone volume fraction demonstrated low effective plastic strain corresponding to strain at failure. The effective plastic strain is not dependent on bone volume fraction due variations on the degree of anisotropy, thus other relevant factors in micro architectural changes should be accounted. Off-axis angle orientation reduces the capability of the trabecular structure to put up with stress during fatigue, thus reduction in fatigue life can be observed during experimental analysis [7,10]. In particular, present work simulated the same behavior of trabecular structure by comparing three different trabecular models orientation. While increment in plastic strain of models in vertical and 45° orientation is found negligible, higher prominent strain is demonstrated by model in horizontal orientation. This is due to the structure of the model in which dominated by thin struts that are susceptible to bending and buckling. The results yielded in present work are in conjunction with previous studies which reported weaker trabecular in transverse orientation with higher shear stress concentration and shorter fatigue life [10,11]. Similar behavior has also been observed in anisotropic reinforced composites, in which demonstrates strength reduction at different fibers orientation [34]. The same observation was also found previously in which demonstrated whole bone sustainability towards higher loading in the main axis, thus different orientation reduced the ability to withstand the load [35,36]. Differences in strains at failure have also been reported to be influenced by geometry [7,15]. Here, direct essentialities are true of providing detailed information on bone properties for improvement in fixation system.

High-resolution FE models can be used to accurately predict the trabecular failure [37,38] and simulate bone fracture [39,40]. However, none of the reported literatures for bone fatigue analysis had involved bulk structure of the trabecular despite the clinical evidences of fatigue failure in the trabecular region. In this section, the presence of periodic boundary on a small unit of bulk trabecular model was analyzed to predict the fatigue life the model with different morphological parameters. The boundary condition was set on the free surface of the model in order to reflect the macroscopic mechanical properties of the trabecular at actual size as in experimental tests. The presence of the boundary reduced the uncertainty in the evaluation of midpoint in trabeculae element to derived tissue properties by von-Mises stress or surface value critical location. The mechanical properties may have been underestimated due to the loss of connectivity and dissimilarity in structure of the model in comparison to the sample used for experimental analyses. Mesh convergence analysis were also carried out. The optimum number of element obtained was about 1,000,000 number of element. The number of elements influenced the prediction accuracy and estimate the duration for system solver. Young’s modulus was underestimated by 63.86% for the analyses with exclusive boundary condition. Several models of trabecular bone with different microarchitecture parameters were inspected in order to compare the effects of periodic boundary in stress-strain distribution under uniaxial and multiaxial loading. The models were first imposed with uniform distribution of periodic boundary.



To calculate the initial modulus of the models, seven units of sub-volume trabecular cell were reconstructed from different samples and computationally analyzed. The Young's modulus obtained were within the range of microscopic trabecular value and comparable to the experimental reports [10,41,42]. The implementation of periodic boundary in FE analyses done in this section has led to infinite domain of trabecular microarchitecture. With implemented periodic boundary, such limitation in developing whole trabecular model as in experimental analyses could be overcome. The process should require advanced imaging technology in order to develop high resolution image for such purpose.

Moreover, the computational analyses would be longer in duration, as opposed to the computational method preferences; cost-effective, non-destructive and timesaving. Most FE analyses of trabecular bone accounted only the apparent properties [15,40,43] and only a few have implemented the periodic boundary on the models tested [44–47]. However, no comparison has ever been made in between uniaxial and multiaxial trabecular fatigue. Back calculated has been the method of choice to predict the elastic modulus in studies involving trabecular bone, thus the internal boundary in domain is considered in fatigue evaluation. Here, calibration is needed for the analysis to be in proportioned to the material fatigue properties.

Uniaxial analysis of material without periodic boundary condition results in shear effects due to bending by high compressive magnitude [48,49]. This in turn demonstrates higher stress and strain difference in comparison to the uniaxial analysis with periodic boundary condition. However, in the analysis under multiaxial loading, the trabecular structure was restricted by shear locking between the interface of periodic boundary condition and the deformed body. Although higher magnitude in analyses without periodic boundary condition is observed in comparison to that of under uniaxial loading, the percentage difference between von-Mises stress with and without periodic boundary condition are significantly lower than that of uniaxial loading. Furthermore, the average difference of volumetric strain evaluation was about 20% in between load cases.

Under multiaxial loading, the trabecular were constrained to tolerate with shear thus restricted the structure from deformation. The contribution of the local von-Mises stress distribution was less in analysis of sample with periodic boundary condition than the sample without periodic boundary condition. In real behavior, this may underestimate the displacement and minimize shear stresses due to the constrained interface. Furthermore, the interfacial surface at some locations was constrained under compression and therefore no further increment in strain was noticed. This behavior was also observed in previous study [36,44]. As the trabecular structure in vivo is confined by cortical bone, net deformations supposed to bear by the trabecular is axial compressive load. However, shear stress has induced bending of the trabecular and severely attacked the structure in oblique and horizontal direction which has introduced high stress distribution to the structure. This phenomenon is rarely seen in vitro as previous assessment accounted for only compressive axial loading [6].

Lesser effect of the trabeculae off-axis orientation is demonstrated under uniaxial loading compared to multiaxial loading in which resulted in lower cycles to failure. Higher load or stress levels resulted in higher stress concentration distribution on the same region. In real trabecular behavior, those may be view as the propagation of micro crack and off-axis orientation of trabeculae normally failed due to micro buckling [10]. Therefore, induce a spurious softening of trabecular structure led to higher displace of global stress of the model and can significantly overestimate the value of apparent strain.

The effect of periodic boundary condition mapping in prediction of the mechanical parameters and fatigue life of trabecular bone were assessed by the means of FE computation. The presence of periodic boundary condition has given significant impact on the results and reduced the time taken for the analysis to be completed due to the large number of elements that were defined to be constraint. The incorporation of multiaxial loading was based on the physiological environment, while imposing periodic boundary localized the trabecular structure as such the trabecular being confined by cortical bone. Localization of stress and strain in FE computational analyses may contribute to the development of biomechanical evaluation. Future work may involve mimicry of in vivo condition with mechanobiological model which include fluid effect on the structural mechanics.

## 5. Conclusion

The resistance of trabecular bone deformation to loading in both uniaxial and multiaxial modes improved the fatigue life and failure with application of periodic boundary condition. The substantial constraint is the reduction on discretization error will reduce time in computation. So it is significant to consider carefully the boundary condition effects when utilizing such a complex multiaxial loading mode. Additionally, multiaxial loading gives distinct effects towards boundary condition compare to uniaxial whereas percentage prediction of fatigue failure is lower and applying of periodic boundary reflect a more precise real loading condition.

Fatigue failure of trabecular bone appears to be dominated by low shear properties and regardless of loading type; trabecular bone still can be failed by shear. Weaker trabecular struts in off-axis to loading orientation is governed by twisting and bending deformation under multiaxial stress condition. The trabecular bone fatigue damage behavior was successfully observed during the increase of strain accumulation. Modulus reduction can be viewed as driving the structural deformation under cyclic loads and incorporate with energy dissipations.

## Acknowledgement

The authors gratefully acknowledge to the Ministry of Education Malaysia for financial supports given under the Fundamental Research Grant Scheme (FRGS/1/2018/TK03/UNIKL/02/4).

## References

- [1] Papakonstantinou M K, Hart M J, Farrugia R, Gosling C, Kamali Moaveni A, van Bavel D, Page R S and Richardson M D 2017 Prevalence of non- union and delayed union in proximal humeral fractures *ANZ J. Surg.* **87** 55–9
- [2] Goff M G, Lambers F M, Sorna R M, Keaveny T M and Hernandez C J 2015 Finite element models predict the location of microdamage in cancellous bone following uniaxial loading *J. Biomech.* **48** 4142–8
- [3] Pisani P, Renna M D, Conversano F, Casciaro E, Di Paola M, Quarta E, Muratore M and Casciaro S 2016 Major osteoporotic fragility fractures: Risk factor updates and societal impact *World J. Orthop.* **7** 171
- [4] Taylor M and Tanner K E 1997 Fatigue failure of cancellous bone: a possible cause of implant migration and loosening *J. Bone Joint Surg. Br.* **79** 181–2
- [5] Goff M G, Lambers F M, Nguyen T M, Sung J, Rinnac C M and Hernandez C J 2015 Fatigue-induced microdamage in cancellous bone occurs distant from resorption cavities and trabecular surfaces *Bone* **79** 8–14
- [6] Rapillard L, Charlebois M and Zysset P K 2006 Compressive fatigue behavior of human vertebral trabecular bone *J. Biomech.* **39** 2133–9
- [7] Dendorfer S, Maier H J, Taylor D and Hammer J 2008 Anisotropy of the fatigue behaviour of cancellous bone *J. Biomech.* **41** 636–41
- [8] Haddock S M, Yeh O C, Mummaneni P V., Rosenberg W S and Keaveny T M 2004 Similarity in the fatigue behavior of trabecular bone across site and species *J. Biomech.* **37** 181–7
- [9] Kinney J H and Ladd A J C 1998 The relationship between three- dimensional connectivity and the elastic properties of trabecular bone *J. Bone Miner. Res.* **13** 839–45
- [10] Fatihhi S J, Rabiatal A A R, Harun M N, Kadir M R A, Kamarul T and Syahrom A 2016 Effect of torsional loading on compressive fatigue behaviour of trabecular bone *J. Mech. Behav. Biomed. Mater.* **54** 21–32
- [11] Fenech C M and Keaveny T M 1999 A cellular solid criterion for predicting the axial-shear failure properties of bovine trabecular bone
- [12] Rincón-Kohli L and Zysset P K 2009 Multi-axial mechanical properties of human trabecular bone *Biomech. Model. Mechanobiol.* **8** 195–208
- [13] Fatihhi S J, Harun M N, Abdul Kadir M R, Abdullah J, Kamarul T, Öchsner A and Syahrom A 2015 Uniaxial and Multiaxial Fatigue Life Prediction of the Trabecular Bone Based on Physiological Loading: A Comparative Study *Ann. Biomed. Eng.* **43** 2487–502
- [14] Kadir M R A, Syahrom A and Öchsner A 2010 Finite element analysis of idealised unit cell cancellous structure based on morphological indices of cancellous bone *Med. Biol. Eng. Comput.* **48** 497–505
- [15] Wolfram U, Gross T, Pahr D H, Schwiedrzik J, Wilke H-J and Zysset P K 2012 Fabric-based Tsai–Wu yield criteria for vertebral trabecular bone in stress and strain space *J. Mech. Behav. Biomed. Mater.* **15** 218–28
- [16] Moore T L a. and Gibson L J 2003 Fatigue of Bovine Trabecular Bone *J. Biomech. Eng.* **125** 761
- [17] Follet H, Boivin G, Rumelhart C and Meunier P J 2004 The degree of mineralization is a determinant of bone strength: a study on human calcanei *Bone* **34** 783–9
- [18] Ganguly P, Moore T L A and Gibson L J 2004 A phenomenological model for predicting fatigue life in bovine trabecular bone *J. Biomech. Eng.* **126** 330–9
- [19] Guillén T, Zhang Q-H, Tozzi G, Ohrndorf A, Christ H-J and Tong J 2011 Compressive behaviour of bovine cancellous bone and bone analogous materials, microCT characterisation and FE analysis *J. Mech. Behav. Biomed. Mater.* **4** 1452–61
- [20] Hsieh Y F and Silva M J 2002 In vivo fatigue loading of the rat ulna induces both bone formation and resorption and leads to time-related changes in bone mechanical properties and density *J. Orthop. Res.* **20** 764–71
- [21] Yamamoto E, Crawford R P, Chan D D and Keaveny T M 2006 Development of residual strains in human vertebral trabecular bone after prolonged static and cyclic loading at low load levels *J. Biomech.* **39** 1812–8
- [22] Turunen M J, Prantner V, Jurvelin J S, Kröger H and Isaksson H 2013 Composition and microarchitecture of human trabecular bone change with age and differ between anatomical locations *Bone* **54** 118–25
- [23] Stauber M and Müller R 2006 Age-related changes in trabecular bone microstructures: global and local morphometry *Osteoporos. Int.* **17** 616–26
- [24] Kopperdahl D L and Keaveny T M 1998 Yield strain behavior of trabecular bone *J. Biomech.* **31** 601–8
- [25] Padilla F, Jenson F, Bousson V, Peyrin F and Laugier P 2008 Relationships of trabecular bone structure with quantitative ultrasound parameters: In vitro study on human proximal femur using transmission and backscatter measurements *Bone* **42** 1193–202

- [26] Jaasma M J, Bayraktar H H, Niebur G L and Keaveny T M 2002 Biomechanical effects of intraspecimen variations in tissue modulus for trabecular bone *J. Biomech.* **35** 237–46
- [27] Kumar D, Manal K T and Rudolph K S 2013 Knee joint loading during gait in healthy controls and individuals with knee osteoarthritis *Osteoarthr. Cartil.* **21** 298–305
- [28] Teo J C M, Si-Hoe K M, Keh J E L and Teoh S H 2007 Correlation of cancellous bone microarchitectural parameters from microCT to CT number and bone mechanical properties *Mater. Sci. Eng. C* **27** 333–9
- [29] Bourne B C and van der Meulen M C H 2004 Finite element models predict cancellous apparent modulus when tissue modulus is scaled from specimen CT-attenuation *J. Biomech.* **37** 613–21
- [30] Harrison N M, McDonnell P F, O'Mahoney D C, Kennedy O D, O'Brien F J and McHugh P E 2008 Heterogeneous linear elastic trabecular bone modelling using micro-CT attenuation data and experimentally measured heterogeneous tissue properties *J. Biomech.* **41** 2589–96
- [31] Legrand E, Chappard D, Pascaretti C, Duquenne M, Krebs S, Rohmer V, Basle M and Audran M 2000 Trabecular bone microarchitecture, bone mineral density, and vertebral fractures in male osteoporosis *J. Bone Miner. Res.* **15** 13–9
- [32] Yeh O C and Keaveny T M 1999 Biomechanical effects of intraspecimen variations in trabecular architecture: a three-dimensional finite element study *Bone* **25** 223–8
- [33] Liu X S, Huang A H, Zhang X H, Sajda P, Ji B and Guo X E 2008 Dynamic simulation of three dimensional architectural and mechanical alterations in human trabecular bone during menopause *Bone* **43** 292–301
- [34] Chawla K K 2013 *Composite materials*
- [35] Thomsen J S, Niklasson A S, Ebbesen E N and Brüel A 2013 Age-related changes of vertical and horizontal lumbar vertebral trabecular 3D bone microstructure is different in women and men *Bone* **57** 47–55
- [36] Ding M, Odgaard A, Linde F and Hvid I 2002 Age- related variations in the microstructure of human tibial cancellous bone *J. Orthop. Res.* **20** 615–21
- [37] Tsubota K, Suzuki Y, Yamada T, Hojo M, Makinouchi A and Adachi T 2009 Computer simulation of trabecular remodeling in human proximal femur using large-scale voxel FE models: Approach to understanding Wolff's law *J. Biomech.* **42** 1088–94
- [38] Majumdar S, Kothari M, Augat P, Newitt D C, Link T M, Lin J C, Lang T, Lu Y and Genant H K 1998 High-resolution magnetic resonance imaging: three-dimensional trabecular bone architecture and biomechanical properties *Bone* **22** 445–54
- [39] Keyak J H 2001 Improved prediction of proximal femoral fracture load using nonlinear finite element models *Med. Eng. Phys.* **23** 165–73
- [40] Shefelbine S J, Augat P, Claes L and Simon U 2005 Trabecular bone fracture healing simulation with finite element analysis and fuzzy logic *J. Biomech.* **38** 2440–50
- [41] Røhl L, Larsen E, Linde F, Odgaard A and Jørgensen J 1991 Tensile and compressive properties of cancellous bone *J. Biomech.* **24** 1143–9
- [42] Nicholson P H F and Strelitzki R 1999 On the prediction of Young's modulus in calcaneal cancellous bone by ultrasonic bulk and bar velocity measurements *Clin. Rheumatol.* **18** 10–6
- [43] Ojanen X, Tanska P, Malo M K H, Isaksson H, Väänänen S P, Koistinen A P, Grassi L, Magnusson S P, Ribbel-Madsen S M and Korhonen R K 2017 Tissue viscoelasticity is related to tissue composition but may not fully predict the apparent-level viscoelasticity in human trabecular bone—An experimental and finite element study *J. Biomech.* **65** 96–105
- [44] Bevell G and Keaveny T M 2009 Trabecular bone strength predictions using finite element analysis of micro-scale images at limited spatial resolution *Bone* **44** 579–84
- [45] van Rietbergen B, Weinans H, Huiskes R and Odgaard A 1995 A new method to determine trabecular bone elastic properties and loading using micromechanical finite-element models *J. Biomech.* **28** 69–81
- [46] Massarwa E, Aboudi J, Galbusera F, Wilke H-J and Haj-Ali R 2017 A nonlinear micromechanical model for progressive damage of vertebral trabecular bones *J. Mech. Mater. Struct.* **12** 407–24
- [47] Haj-Ali R, Massarwa E, Aboudi J, Galbusera F, Wolfram U and Wilke H-J 2017 A new multiscale micromechanical model of vertebral trabecular bones *Biomech. Model. Mechanobiol.* **16** 933–46
- [48] Radzuan N A M, Sulong A B, Mamat M R, Tharazi I, Tholibon D, Dweiri R and Hammadi M S 2018 Kenaf Reinforced PLA Composite Thermoforming: A Numerical Simulation *Int. J. Integr. Eng.* **10**
- [49] Zakwan F A A, Krishnamoorthy R R, Ibrahim A and Ismail R 2018 A Finite Element (FE) simulation of naked solid steel beam at elevated temperature *Int. J. Integr. Eng.* **10**